Nuclear Engineering and Design 333 (2018) 76–86

Contents lists available at ScienceDirect

Nuclear Engineering and Design

journal homepage: www.elsevier.com/locate/nucengdes

Numerical methodology for fluid-structure interaction analysis of nuclear fuel plates under axial flow conditions

Javier González Mantecón*, Miguel Mattar Neto

Instituto de Pesquisas Energéticas e Nucleares, IPEN-CNEN/SP, Av. Prof. Lineu Prestes, 2242 – Cidade Universitária, CEP 05508-000 São Paulo, SP, Brazil

ARTICLE INFO

Keywords:
Plate-type fuel element
Fluid-structure interaction
Critical velocity
Research reactor
Hydroelastic instability

ABSTRACT

Shell-type fuel elements are widely used in nuclear research reactors. The nuclear fuel is contained in parallel shells, flat or curved, that are separated by narrow channels through which the fluid flows to remove the heat generated by fission reactions. A major problem of this fuel assembly design is the hydraulic instability of the shells caused by the high flow velocities. The objective of the study presented here is the development of a fluid-structure interaction methodology to investigate numerically the onset of hydroelastic instability of flat-shell-type fuel elements, also known as plate-type fuel assemblies, under axial flow conditions. The system analyzed consists of two nuclear fuel plates bounded by three-equal coolant channels. It is developed using the commercial codes ANSYS CFX for modeling the fluid flow and ANSYS Mechanical to model the plates. The fluid-structure interaction methodology predicts a behavior consistent with other theoretical and experimental works. Particularly, the maximum deflection of the plates is detected at the leading edge and it is a linear function of the square of the fluid velocity up to the Miller's theoretical value. For velocities above this value, a nonlinear relationship is observed. This relationship indicates that structural changes are taking place in the plates. Furthermore, for fluid velocities greater than the Miller's velocity, an extra deflection peak is observed near the trailing edge of the plates. Thus, structural alterations also happen along the length of the flat-shells.

1. Introduction

Shell-type fuel elements are widely used in nuclear research reactors. The nuclear fuel is contained in parallel shells, flat or curved, that are separated by narrow channels through which the fluid flows to remove the heat generated by fission reactions. These shells have to be thin enough to prevent excessive internal temperature generation and yet strong enough to maintain stable configuration. A major problem of this fuel assembly design is the hydraulic instability of the shells caused by the high fluid velocities.

One of the first published reports regarding flow induced deflection in a shell-type fuel element was written by Stromquist and Sisman (1948). The study was performed in a mockup and it was found that when the coolant velocity was raised to sufficiently high values, fuel shells deformed plastically. In 1958, the same problem was detected by Ronald Doan during the fuel element design, development and construction for incorporation into the Engineering Test Reactor (ETR). Doan qualitatively discussed a critical flow field related to the onset of plastic deformation of the fuel shells (Doan, 1958). Later, Daniel Miller used the Doan's hypothesis and established a method to determine the maximum velocity that a series of shells, flat or curved, with fixed sides can sustain before collapse (Miller, 1958). This velocity is also known as "Miller's critical velocity". His analysis gives a basic idea of how the shells within a fuel assembly tend to deflect. Adjacent shells move in opposite directions at high flow rates, causing alternate closing and opening of the coolant channel. The main limitation of the Miller's method is that the 3D effects of the system are neglected. However, up to the present, it is applied during the design of new fuel elements.

Flat-shell-type fuel element, also known as plate-type fuel element, has been studied more than any other geometric shape due to its vulnerability to failure and its relatively weak structural capabilities with respect to other geometric forms (Marcum, 2014). The major part of the studies have been conducted by using analytical and experimental methods (Alvim de Castro, 2017; Cekirge and Ural, 1978; Davis and Scarton, 1985; Groninger and Kane, 1963; Guo and Païdoussis, 2000; Howard et al., 2015; Jensen and Marcum, 2014; Johansson, 1959; Kim and Davis, 1995; Li et al., 2012; Liu et al., 2011; Pavone and Scarton, 1983; Scavuzzo, 1965; Smissaert, 1969, 1968; Smith, 1968; Swinson et al., 1995; Swinson and Yahr, 1990; Weaver and Unny, 1970).

In the last years, the Computational Fluid Dynamics (CFD) and Finite Element Analysis (FEA) techniques have demonstrated its feasibility and potential to solve many industrial issues. However, few

* Corresponding author.
E-mail address: javier.mantecon@ipen.br (J. González Mantecón).

https://doi.org/10.1016/j.nucengdes.2018.04.009
Received 6 November 2017; Received in revised form 9 February 2018; Accepted 9 April 2018
Available online 24 April 2018

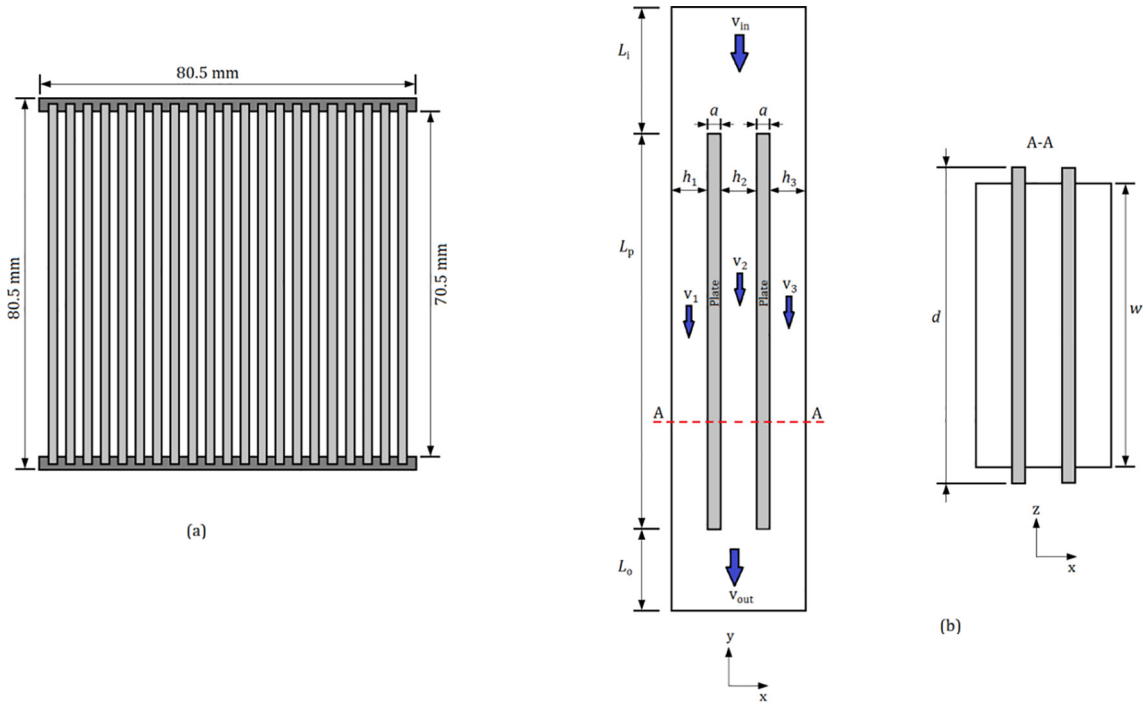

Fig. 1. Top view of the standard fuel element (a) and schematic diagram of the domain under consideration (b).

Table 1
Geometric specifications and material properties.

Parameter	Value
Coolant channel thickness, h [mm]	2.45
Plate thickness, a [mm]	1.35
Coolant channel width (wetted plate width), w [mm]	70.5
Plate width, d [mm]	75
Inlet length, L_i [mm]	190
Coolant channel (plate) length, L_p [mm]	655
Outlet length, L_o [mm]	70.0
Fluid properties (Water)	
Density, ρ [kg/m^3]	997.561
Dynamic viscosity, μ [Pa·s]	8.887e-4
Plate properties (Aluminum Alloy 6061-T6)	
Density, ρ_p [kg/m^3]	2700
Young's modulus, E [GPa]	68.9
Poisson's ratio, υ	0.33
Tensile yield strength, σ_y [MPa]	276

investigations concern fluid-structure interaction (FSI) problems in plate-type fuel assemblies by applying these techniques. After a deep search, the authors can list a reduced number of references with direct relevance to the subject discussed (Curtis et al., 2013; Jesse, 2015; Kennedy and Solbrekken, 2011; Kennedy, 2015). These studies were restricted to model a single plate with flow channels on either side. According to Smissaert, the presence of neighboring plates affects the lift force acting on the inlet edge (Smissaert, 1969). Therefore, in this work, we present a numerical analysis using more than one plate, which allows us to consider that effect.

The main objective of the study presented here is the development of a fluid-structure interaction methodology to investigate numerically the onset of hydroelastic instability of plate-type fuel elements under axial flow conditions. An additional purpose is to further the understanding of the behavior of the plates in fluid media and assess how its mechanical stability is related to the hydraulic loads. The FSI model consists of two fuel plates bounded by three coolant channels. It is developed using the commercial CFD code ANSYS CFX for modeling the fluid flow and the FEA code ANSYS Mechanical to model the plates. It is important to highlight that this methodology assists greatly in gaining insights of fluid-structure interaction problem in fuel elements of research reactors, allowing the analysis of complicated geometries under different conditions that would be costly to investigate experimentally. This methodology is important for updating the current analysis techniques applied to research reactor cores design.

2. Multi-field simulations

Fluid-structure interaction is a two field problem: one fluid flow and one structural field. On the one hand, the fluid field results in the load on the solid structure and is thereby a driving force. On the other hand, the structure reacts by means of stresses and deformations to the fluid field. The resulting deformation of the solid field has an impact on the fluid field that has to adapt to the modified boundary (Rao, 2003).

Solution strategies for FSI simulations are mainly divided into monolithic and partitioned methods; this work focuses only on partitioned methods. In the partitioned strategy, the fluid and structure subproblems are solved iteratively. This requires two codes: one for solving the fluid equations and the other for the structural part. This technique is further divided into two categories: one-way and two-way coupling (ANSYS Inc., 2017a).

The method used here is the two-way coupling between ANSYS CFX and ANSYS Mechanical (Transient Structural module). Fluid and solid domain/physical models are created in the ANSYS CFX-Pre and ANSYS Mechanical user interfaces, respectively. Coupling data transfers and controls are specified in the ANSYS CFX-Pre. Both have unlike meshing requirements and different meshes can be generated for the fluid field and the solid field. The meshes must not be equal at the interface but must consist of the identical geometric surface. During two-way coupling calculations, both solvers execute the simulation throughout a sequence of multi-field time steps, each of which consists of one or more coupling iterations. The FEA solver acts as a coupling master process to which the CFD solver connects. Once the connection is established, the solvers advance through a sequence of pre-defined synchronization points (SPs). At each of these SPs, information is exchanged between the solvers (ANSYS Inc., 2017a). This process of data sharing between structure and fluid field continues till the required conditions are satisfied.

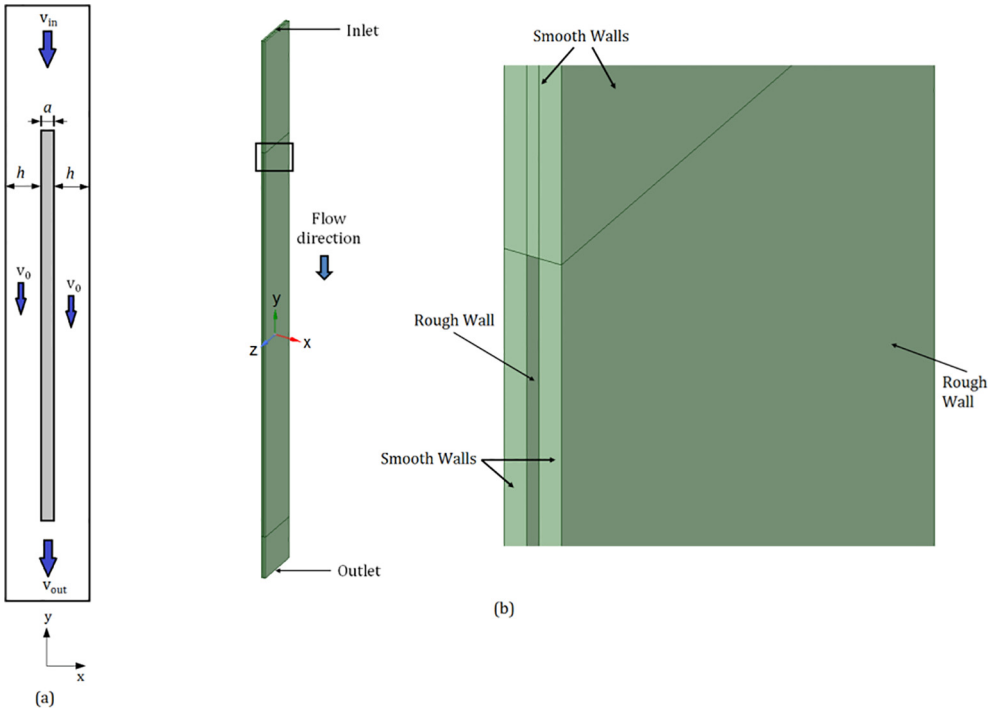

Fig. 2. Schematic diagram of the fluid domain for verification (a) and CFD model (b).

Table 2
Details of meshes in the fluid model verification.

Mesh	Number of elements along edge						Total
	L_i	L_p	L_o	w	h	a	
1 – Fine	80	200	50	52	16	16	657,280
2 – Coarse	57	141	35	37	11	11	227,106

Table 3
Results of CFD mesh sensitivity analysis.

Metric	Mesh 1	Mesh 2	Error
ΔP	101122.54 Pa	101849.66 Pa	0.71%
τ_w	182.36 Pa	183.25 Pa	0.49%

When setting up the FSI simulation, two options are available: explicit and implicit. In explicit coupling, one exchange of data between the fluid and solid domain for each simulation time step is completed. This technique works well for simulations where time precision is not essential. In contrast, in implicit coupling, the codes exchange data many times during a time step. This technique has greater potential for time-accurate solutions but there is a substantial increment in computational time (Pozarlik and Kok, 2007). Since this work is concerned with the static and steady-state deformation of the fuel plates, the explicit coupling scheme is the preferred alternative.

3. Computational setup

In experimental research works were detected flow induced deflections at the leading edge of the plates and along their length. These

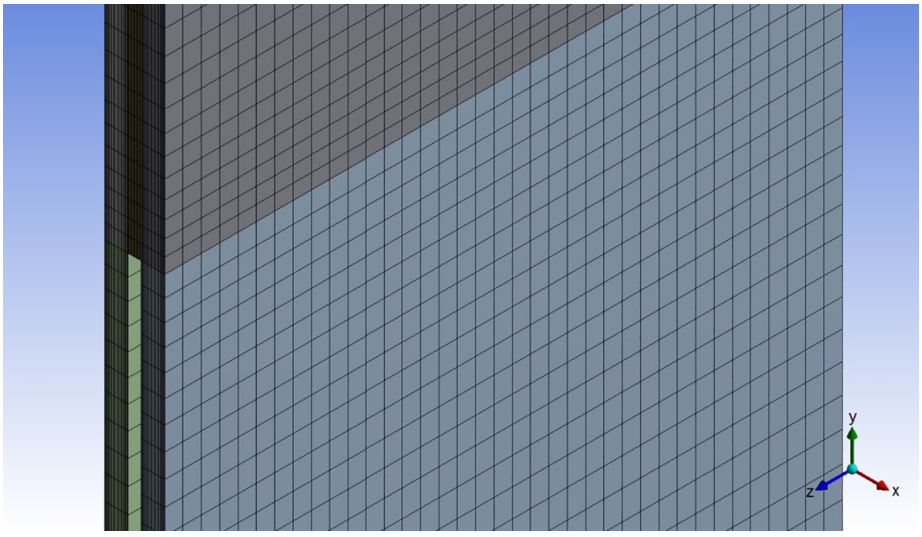

Fig. 3. Coarse mesh used in the CFD model verification.

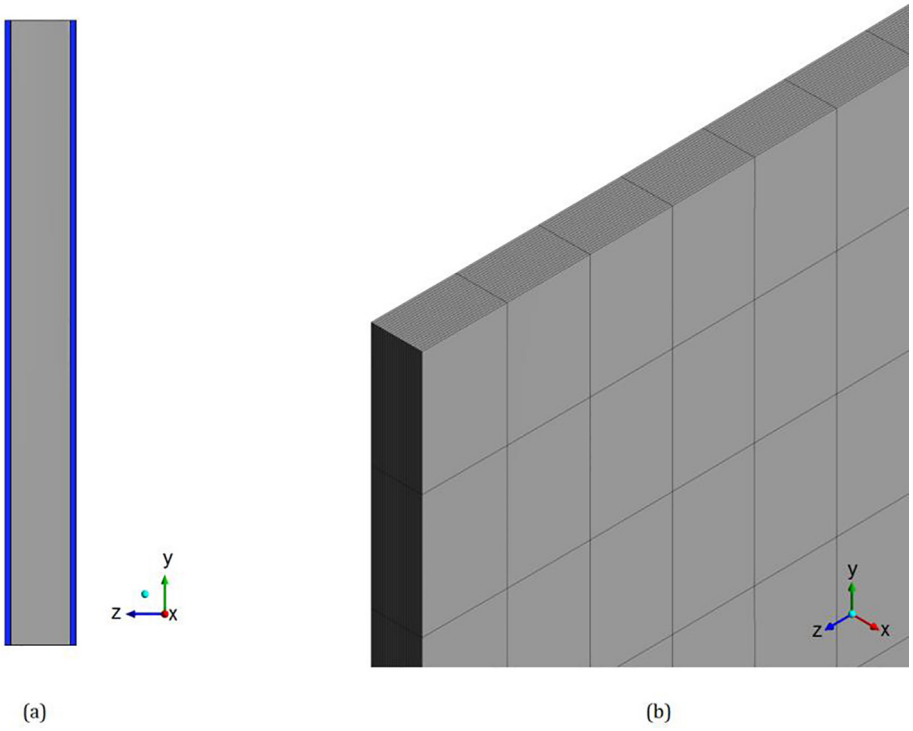

Fig. 4. Plate geometry (a) and a close view of the plate mesh taken at the plate leading edge (b).

Table 4
Details of meshes in the structural model verification.

Mesh	Number of elements along edge			Total
	L_p	d	a	
1 – Fine	200	34	22	149,600
2 – Coarse	200	24	16	76,800

deflections were observed even at fluid velocities lower than the Miller's critical velocity (Groninger and Kane, 1963; Johansson, 1959; Kennedy, 2015; Smissaert, 1968; Smith, 1968; Swinson et al., 1995; Swinson and Yahr, 1990). The deflection that occurs at the leading edge was defined by Smissaert (1968) as static divergence of the class A instability (Benjamin, 1963). It physically means "that the plate will statically deflect until the elastic restoring force cancels the hydrodynamic pressure perturbation". Furthermore, Smissaert concluded that the deformation of fuel plates is a result of pressure differences in the channels between these plates. These pressure differences are originated from the static divergence of the leading edges and from the plate deflections beyond the leading edge.

Taking into consideration those earlier research works, we developed a non-linear fluid-structure interaction analysis to capture both structural response cases, the static divergence at the inlet edge and plate deflection along its length.

3.1. Domain description

The model is built considering the geometric and hydraulic parameters of the future Brazilian Multipurpose Reactor (RMB by its acronyms in Portuguese). The RMB is a 30 MW pool-type research reactor utilizing beryllium and heavy water as reflector, and it is cooled and moderated by light water. The core is a 5 × 5 matrix, containing 23 MTR fuel elements. Each standard fuel assembly has 21 fuel plates that

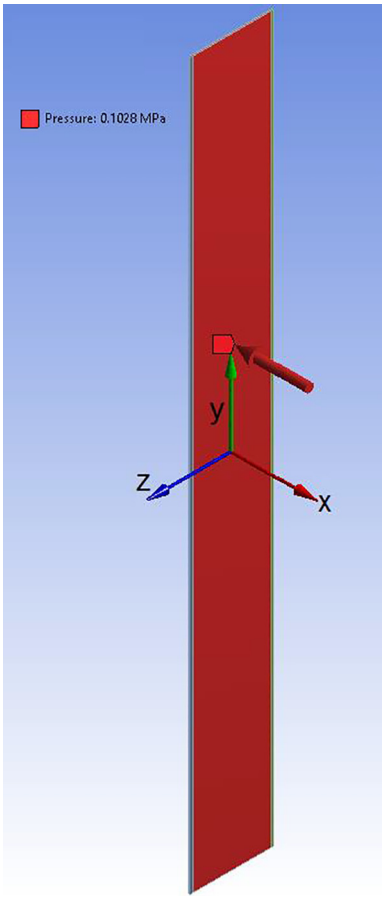

Fig. 5. Uniform pressure load applied on the plate surface.

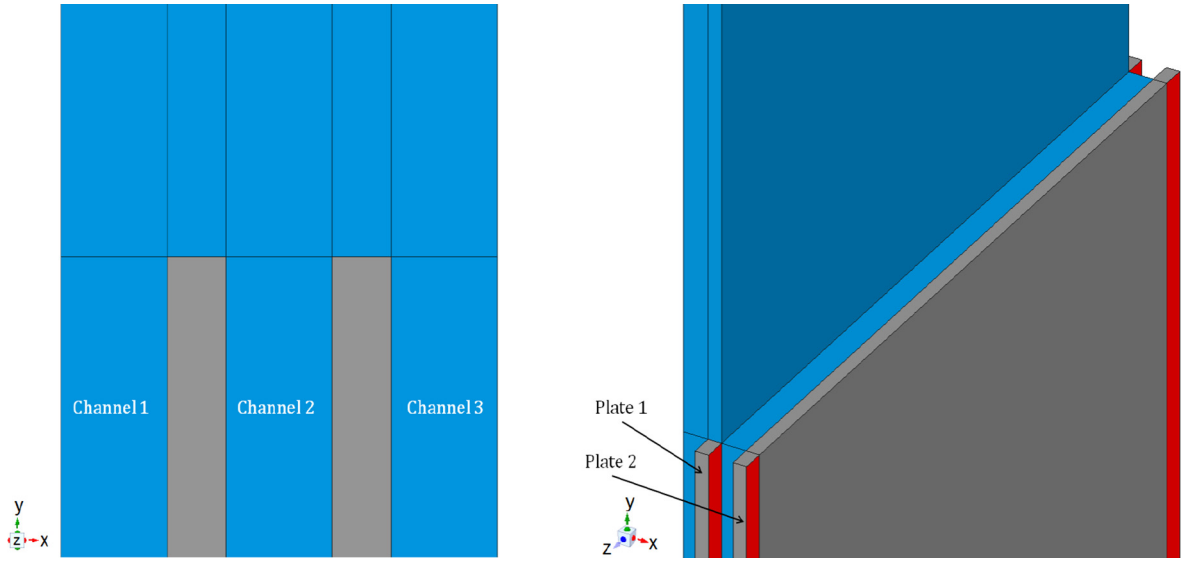

Fig. 6. Fluid-structure interaction model.

Table 5
Settings of the FSI model used in the present work.

Analysis type	• CFX: ANSYS MultiField Coupling • Mechanical: Transient Structural module, large deformations enabled
Material	• Fluid: Water • Solid: Aluminum Alloy 6061-T6
Turbulence model	• Standard k-ε with Scalable Wall Function
Boundary conditions	• v_{in} at the inlet • Zero pressure at the outlet • Fluid-solid interface for the surfaces of the plates in contact with fluid • No-slip rough walls for plate surfaces and surfaces parallel to plates (imitating adjacent plates) • No-slip smooth walls for the remaining surfaces • Zero displacements for the clamped regions of the plates
Mesh	• Fluid: hexahedral, 1,040,000 elements • Solid: hexahedral, 299,200 elements, SOLID186
Convergence criteria	• RMS residuals of all conservation equations < 1e-4 • Imbalances of mass and momentum < 1% • Global variables do not change over iterations • Mesh displacement residual target < 1e-4
Transient scheme	• Second order backward Euler
Coupling scheme	• Explicit
Transfer direction	• Forces: Fluid → Solid • Displacements: Solid → Fluid
Coupling data transfer	• Under relaxation factor = 0.75 • Convergence target = 0.01
Solution sequence	• Solve Mechanical fields before CFX fields

Table 6
Effect of time step on the Point 1 total displacement.

Δt	Total Displacement (Point 1)	Error
0.1 s	0.02301 mm	
0.025 s	0.02292 mm	0.39%

comprise the U_3Si_2-Al fuel meat and the Aluminum Alloy 6061-T6 cladding (Perrotta and Soares, 2015).

Fig. 1 illustrates a top view of the standard fuel assembly and a drawing of the domain under consideration: two fuel plates and three-equal coolant channels. In the figure, the blue arrows indicate the coolant flow direction. Basic specifications of the domain are given in Table 1.

Table 7
Coolant velocities considered in the simulations.

v_0/v_M	v_0 [m/s]	v_{in} [m/s]
≈ 0.5	8.2	6.00
0.6	10.10	7.39
0.7	11.79	8.62
0.8	13.47	9.85
0.9	15.16	11.09
1.0	16.84	12.32
1.1	18.52	13.55
1.2	20.21	14.78

3.2. Mesh generation and verification

Before carrying out the FSI simulations, verification test needs to be done to ensure that the numerical model is sufficiently accurate for the intended use. During the verification different meshes are tested and the numerical solution is compared to an accurate solution of the problem (Oberkampf and Roy, 2010). In this work, the fluid and solid models are verified independently.

3.2.1. Fluid model

For verification purpose, a reduced computational domain is built with two-equal coolant channels and one plate centered (see Fig. 2a). In this figure, the gray area is the position where the fuel plate is located but, during this stage of the work, it is an "empty region". The standard k-ε turbulence model is used. It has been utilized extensively in studies involving narrow channels with very accurate results (Andrade et al., 2015; Gong et al., 2015; Salama et al., 2015). In this paper, the range of y^+ is between 30 and 100, which is in the appropriate range for using Standard Wall Function to treat the near-wall calculation (Salim and Cheah, 2009). The wall y^+ is the ratio between the turbulent and laminar influences in a cell. It is the dimensionless normal distance from the wall (ANSYS Inc., 2017a).

Fig. 2b shows the fluid domain. A uniform velocity is defined as inlet boundary condition. At the outlet, the pressure outlet boundary condition with zero gauge pressure is employed. Velocity at the inlet is set using Eq. (1), taking into account an incompressible fluid and the law of conservation of mass. The average fluid velocity through the

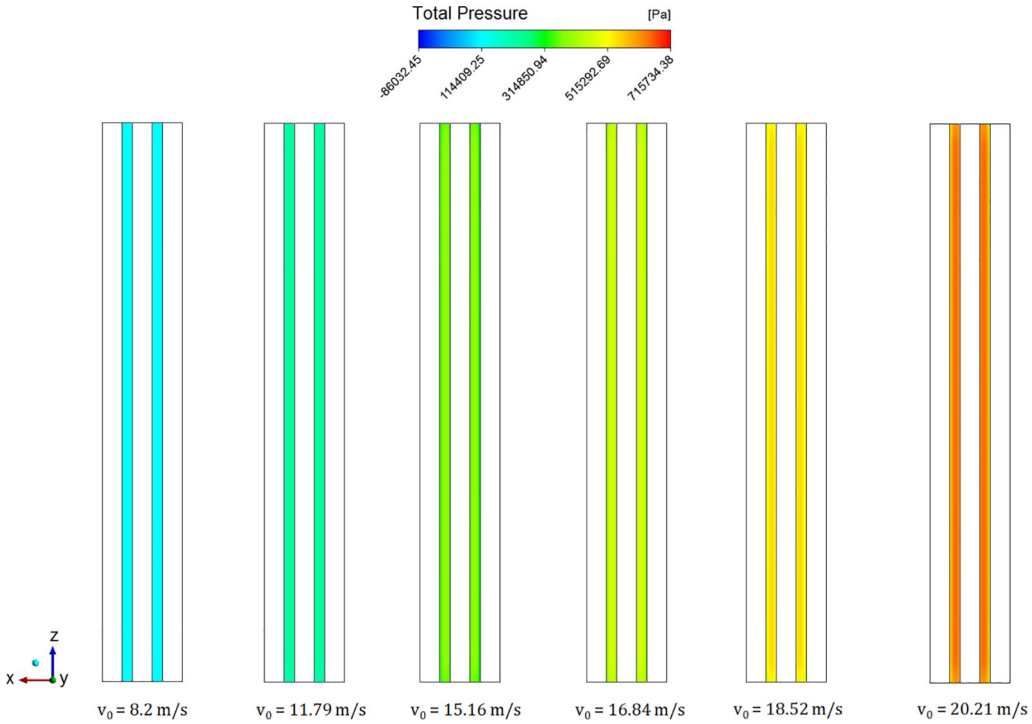

Fig. 7. Pressure contour on the leading edges for different coolant velocities. Fluid flow is entering to the page plane. Plates are considered undeformed.

channels is $v_0 = 8.2$ m/s and hereinafter it is called the "fluid velocity". It is the minimum coolant velocity required in the channels in order to meet the RMB design criteria (INVAP, 2013). The "empty region" surfaces and the surfaces parallel to this region are prescribed as no-slip rough walls. The remaining surfaces are set as no-slip smooth walls.

$$v_{in} = \frac{2h}{2h + a} v_0 \tag{1}$$

The domain is partitioned into different volumes allowing the creation of structured hexahedral meshes. In an effort to capture the contraction/expansion effects at the leading/trailing edges of the plate, a bias factor 4:1 is set up for spacing the cells along the inlet, outlet, and channel lengths. The same bias factor[1] is adopted for the elements along the thickness of the channels. Two different meshes are investigated and Table 2 details the number of cells in all directions. Fig. 3 shows a view of the mesh close to the leading edge of the "empty region".

A high-resolution scheme with first order for the turbulence and a residual target of 1e-5 is used as convergence criterion (ANSYS Inc., 2017a). Another important criterion to confirm the solution convergence is the net mass imbalances. The net mass imbalance to be deemed converged should be less than 0.1%. Besides, the standard initialization method is considered and the initial values are computed from the inlet boundary condition.

To verify the CFD model, a simple 1D correlation is derived to predict the pressure drop across the coolant channel (plate region). It is established by accounting the pressure drop from flow contraction at the leading edge, flow expansion at the trailing edge of the plate, and due to frictional losses (White, 2011). The correlation for the pressure drop is given by the following equation:

$$\Delta P = \frac{\rho v_0^2}{2}\left[0.42\left(1-\frac{D_{h,o}^2}{D_{h,i}^2}\right) + \left(1-\frac{D_{h,i}^2}{D_{h,o}^2}\right)^2 + f\frac{L_p}{D_{h,ch}}\right] \tag{2}$$

where $D_{h,i}$ and $D_{h,o}$ are the hydraulic diameters at inlet and outlet of the form loss junction (expansion/contraction region), correspondingly; $D_{h,ch}$ is the hydraulic diameter of the coolant channel, f is the friction factor in that region and it is solved using the Colebrook formula (White, 2011):

$$\frac{1}{\sqrt{f}} = -2\log\left[\frac{2.51}{Re\sqrt{f}} + \frac{\varepsilon/D_h}{3.7}\right] \quad \text{for } Re > 3000 \tag{3}$$

In the above equation, $\varepsilon = 0.1$ μm is the wall roughness and Re is the Reynolds number.

All simulations are run using the steady-state option. Two variables are selected for the CFD mesh sensitivity: pressure drop across the coolant channel and wall shear stress (τ_w). Results are shown in Table 3. As can be seen from the table the relative errors between the solutions of both meshes are less than 1%. The value of the pressure drop predicted by the 1D correlation is 101490.76 Pa. The difference between the numerical solution using the finest mesh and the value predicted by the correlation is approximately 0.36%. Hence, the mesh with 657,280 elements is sufficiently fine to provide accurate results for the present study. Therefore, similar mesh is adopted for the fluid domain in the multi-field model. In a prior paper, which can be consulted as additional material, the authors presented a detailed sensitivity study that was performed for verifying the CFD model with different turbulence models and an equal fluid flow discretization to that utilized here (González Mantecón and Mattar Neto, 2017).

3.2.2. Plate model

The solid model is depicted in Fig. 4a. Plate material and dimensions are listed in Table 1. Blue surfaces (2.25 mm each one) are the regions used for fixing the plate and the applied boundary condition on front and back surfaces are set to $x = y = z = 0$. Since these surfaces are fixed, the plate is restricted from rotating, and a clamped boundary condition is created. The leading and trailing edges are free, and with the remaining surfaces form the loaded surfaces, which are where pressure loadings are applied.

The plate is discretized using a structured mesh with SOLID186 elements. SOLID186 is a higher-order 3-D 20-node solid element that exhibits quadratic displacement behavior. It is defined by 20 nodes having three degrees of freedom per node and it supports plasticity,

[1] Bias factor: ratio of the longest division and the shortest division.

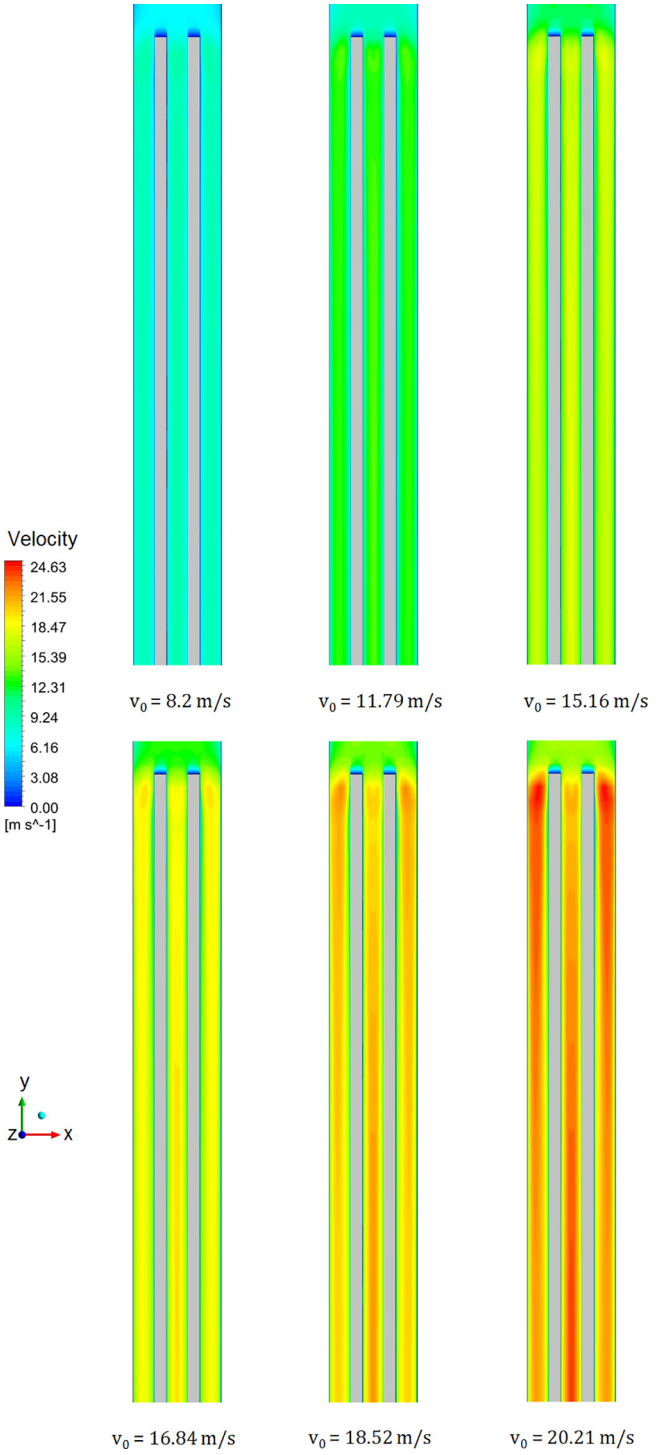

Fig. 8. Velocity contour at mid–plane of coolant channels and close to the leading edges for different fluid velocities. Fluid flow is downward and the plates are considered undeformed.

hyperelasticity, creep, stress stiffening, large deflection, and large strain capabilities (ANSYS Inc., 2017b). A mesh sensitivity analysis is completed to examine the possible dependence of the solution on the mesh size (see Table 4). Fig. 4b shows a closer look at the mesh. The plate is initially undeformed and over one of its surfaces, a uniform pressure load (P) is applied. It imitates the hydraulically induced load that the plate is subjected when it is coupled with the fluid flow. This pressure load is taken from the model in Section 3.2.1 and it is applied at the surface centerline (see Fig. 5).

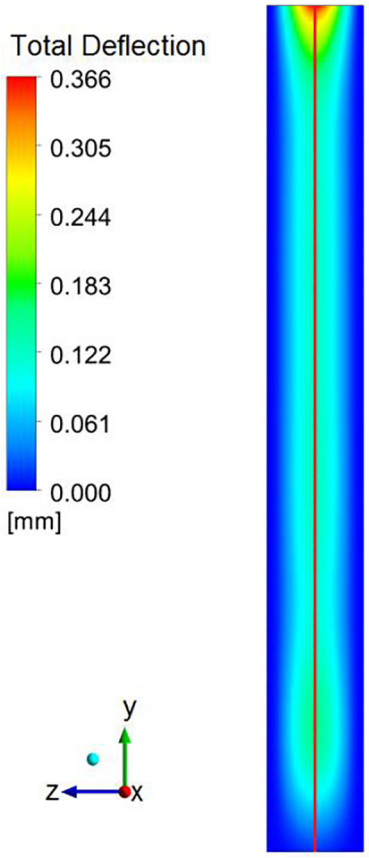

Fig. 9. Path for axial deflection profile extraction of Plate 1 at v_0 = 20.21 m/s. Fluid flow is downward.

An analytical model of the plate is built to verify the numerical model. In view of the fact that the plate is both thin and very long, it is discretized longitudinally creating equally spaced beams. After that, each beam is modeled using simple wide beam theory (Timoshenko and Woinowsky-Krieger, 1959). At the midpoint of the plate the deflection can be calculated using the next equation:

$$\Delta x = \frac{Pw^4\,(1-\upsilon^2)}{32Ea^3} \tag{4}$$

In the mesh sensitivity study, when the number of elements is increased from 76,800 to 149600, the solutions of the deflection differ by approximately 0.34%. Additionally, the deviation of the numerical solution from the analytical result (Δx = 0.4172mm) is 2.57%. This deviation is likely due to solver accounting for the non-linearity and 3D effects that are present when a plate bends. Nonetheless, this result verifies the capability of the numerical model to obtain accurate solutions of plate deflection. Twenty-two 3D elements along the thickness for describing thin plates are enough to capture their flexural behavior with a high degree of accuracy. Hence, the 149,600 elements mesh is chosen for further simulations.

3.3. Fluid-structure interaction model

As mentioned previously, the computational domain considered in the FSI model is composed of two fuel plates and three coolant channels (see Fig. 1). Fig. 6 shows the combined solid and fluid models. Plates are represented by gray volumes, while the fluid is shown in blue. On the right-hand side of the image, the domain has been cut out, so that, one of the plates is visible. The plate and fluid meshes are based on the studies in the preceding sections.

For the multiphysics model, the velocity at the inlet is defined as

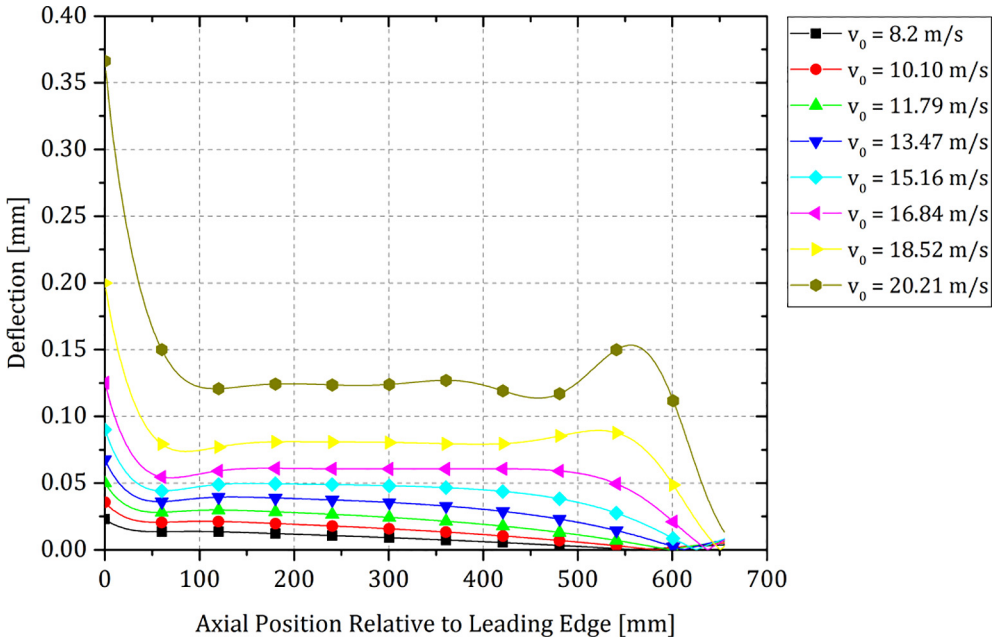

Fig. 10. Axial deflection profile of Plate 1 at various fluid velocities.

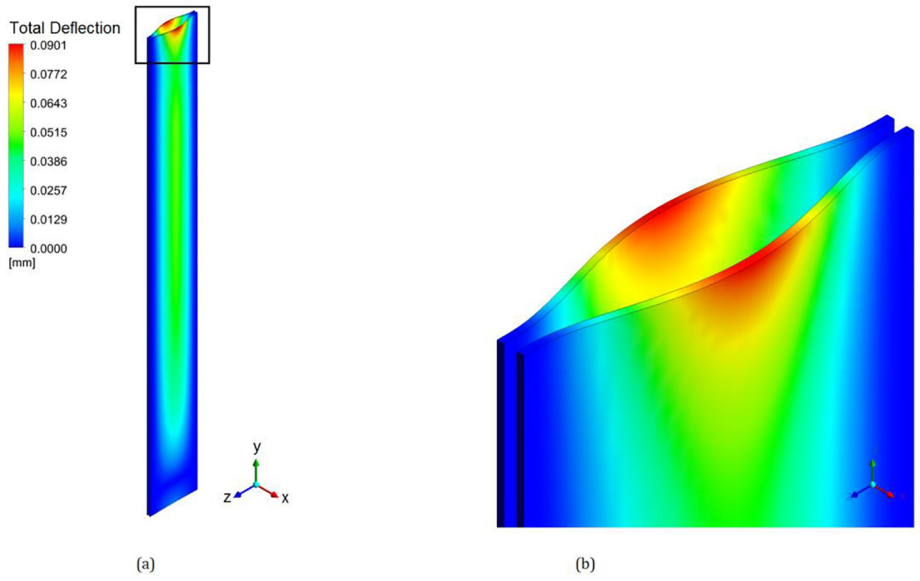

Fig. 11. Deflection of the plates (a) and a close view at the leading edges (b) at v_0 = 15.16 m/s. Fluid flow is downward. Deflection scale factor of 0.5×.

follows:

$$v_{in} = \frac{3h}{3h + 2a} v_0 \quad (5)$$

Table 5 summarizes some parameters in the FSI model settings. The FSI effect requires both the fluid and the solid analysis to be transient. Hence, in order to get a good balance between computational efficiency and stability, it is critical to determine a suitable time step size. A study on the impacts of the time step size in the multi-field simulations is discussed in the next subsection.

3.3.1. Time step selection

In transient FSI analysis, the fluid model time step must be equal to the FSI time step, while a smaller value can be used for the structure model time step. This so-called sub-cycling is sometimes required to improve stability (Du, 2010), but the utilization of different time steps leads to increase the calculation time. That's why in this work, the criterion for selecting an adequate time step is to consider a unique time step that ensures a good balance between computation time and solution accuracy.

A time step dependency study is carried out in terms of displacement amplitudes. Using the FSI model, simulations are completed considering the fluid at 8.2 m/s and Δt of 0.1 and 0.025 s. The transient cases are run for 1.5 s. At the center of the Plate 1 leading edge, a monitor point (Point 1) is located and its total displacement is extracted and listed in Table 6. Finally, with the displacements, relative errors are estimated. From the table, it can be concluded that Δt = 0.025 s is sufficient to deliver accurate results.

4. Results and discussion

Simulations were completed to examine the behavior of the plates under axial flow conditions. In Table 7 the fluid velocities for the numerical simulations are shown. Firstly, the RMB design velocity was

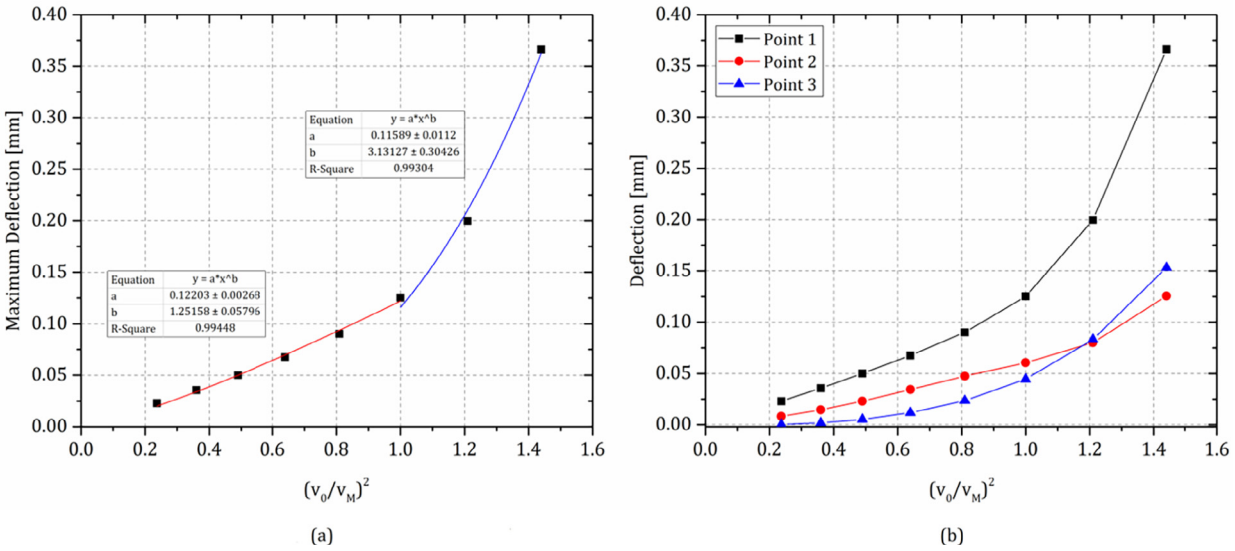

Fig. 12. Maximum deflection at the leading edge (a) and plate deflections at different positions (b). Point 1 is located at the center of the leading edge, Point 2 at the center of the plate and Point 3 at 100 mm from the trailing edge.

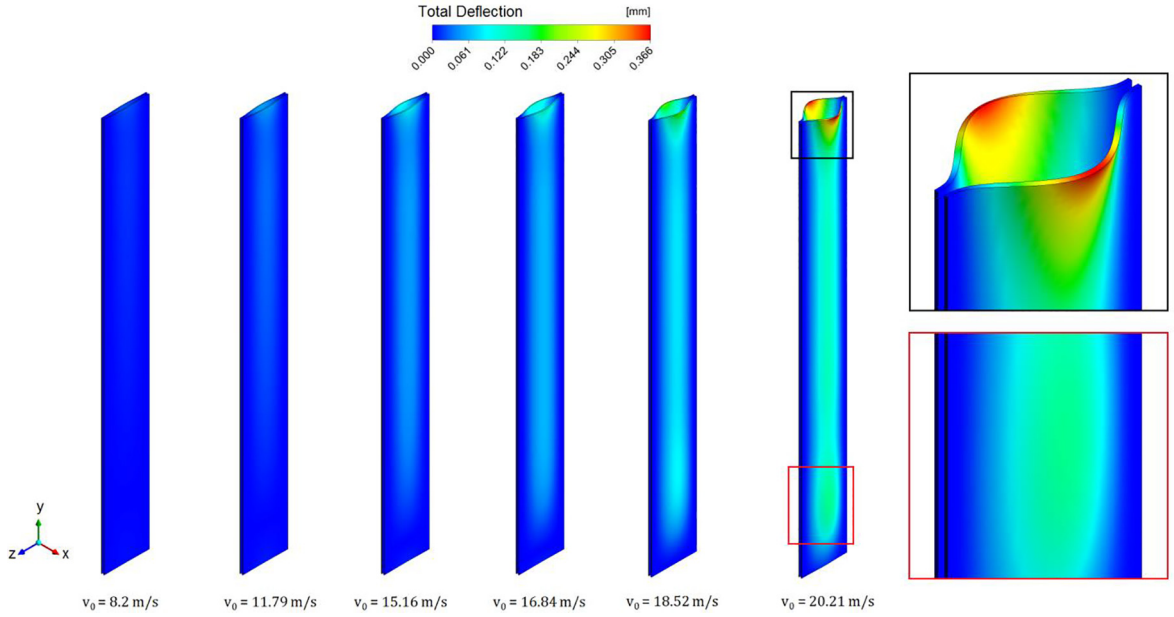

Fig. 13. Deflection contours of the plates for different fluid velocities. Fluid flow is downward. Deflection scale factor of 0.5x.

used and the deflection of the plates was calculated. Afterward, using this result as initial condition, static deflections were obtained at fluid velocity ratios v_0/v_M equal to 0.6, 0.7, 0.8, 0.9, 1.0, 1.1 and 1.2. The Miller's velocity of this assembly is $v_M = 16.84$ m/s and it is given by Eq. (6). It should be mentioned that each simulation was performed on an Intel Xeon dual processor E5-2640 family PC, 2.00 GHz, with 48 GB of RAM.

$$v_M = \sqrt{\frac{15Ea^3h}{\rho w^4 (1-v^2)}} \tag{6}$$

Fig. 7 shows a color plot of the pressure distribution on the surface of the leading edges for different fluid velocities. The contours of the velocity magnitude at mid-plane of coolant channels and near the inlet edges are provided in Fig. 8. As it is expected, the increase of the coolant velocity leads to raising the pressure on these surfaces.

The deflection profile of the fuel plates was extracted along the axial centerline. A path was created on one surface of the plates from the leading edge to the trailing edge. An example of this process is shown in Fig. 9. The red line indicates the path for deflection profile extraction.

As equal coolant channels and equal fuel plates are studied, identical deflections were obtained for both plates. For this reason, only the Plate 1 deflection profile is shown in Fig. 10. As expected, with the flow rate increment, the resulting pressure on the plates and deflection also increase. The maximum deflection happened at the leading edge of the plates. Besides, the analyses demonstrated that leading edge divergence can occur below the Miller's velocity. In the figure it is possible to observe, close to the trailing edge, a region of incremented deflection that begins to appear with the rising of fluid velocity.

Fig. 11 depicts the total deflection of both fuel plates from the 15.16 m/s simulation. It is demonstrated that the displacement of the plates is in opposite directions. However, in a complete assembly where there are more than two fuel plates, adjacent plates can deflect in the same direction and, consequently, to close the coolant channel. In that case, large deflections could cause flow redistribution, resulting in

overheating and/or Departure from Nucleate Boiling phenomenon.

The maximum deflection of the plates has also been plotted versus the square of the velocity ratio in Fig. 12a. From the equation of motion for a flat plate, it is known that the plate deflection is related to pressure forces acting on its surface (Weaver and Unny, 1970). In addition, the fluid-dynamic pressure over the plate is proportional to the fluid velocity squared. Thus, for evaluation purposes and to determine the onset of the hydroelastic instability, we related the static deflection at the leading edge versus the fluid velocity squared. It is important to declare that the relationship between plate deflection and velocity squared had been previously used by other authors (Johansson, 1959; Smissaert, 1968).

In Fig. 12a, the graph incorporates two power law curves that fit the points. The first curve (red line), taking velocities less than and equal to 16.84 m/s, suggests that the deflection is a linear function of the square of the fluid velocity. In contrast, at higher velocities (> 16.84 m/s), the relationship becomes increasingly more nonlinear (blue line). This different relationship is an indication that structural changes are taking place in the plates. Then, the point where there is a change of curve shape is associated with the onset of the hydroelastic instability. In this case, that point is coincident with the Miller's velocity. On the other hand, in Fig. 12b the plate deflections at the leading edge center (Point 1) and two extra locations are presented. Point 2 was positioned at the center of the plate and Point 3 at 100 mm from the trailing edge. It should be noted that, in Point 3, the plate deformed more rapidly at velocities above the Miller's theoretical value, analogous to how it deflects at the leading edge.

Deflection contour plots of the plates for different fluid velocities are shown in Fig. 13. Comparing these contours it is possible to notice the change in plate profile. As it was indicated previously, at $v_0 = 20.21$ m/s the model predicts two distinct peaks, the first at the leading edge and the second near the trailing edge. This result shows that, in addition to the leading edge divergence, deflections can also occur along the length of the plates for velocities greater than the Miller's velocity. Hence, the safe operation of the fuel assembly can be compromised with the deflection of the fuel plates.

5. Conclusions

In this work, a fluid-structure interaction methodology for predicting the onset of hydroelastic instability of plate-type fuel assemblies was developed, by coupling CFD and FEA codes. The coupling strategy was based on the two-way fluid-structure interaction method, in which the fluid loads calculated by CFD modeling are sent to FEA model as boundary conditions and the displacements of the structure are transferred back to the CFD analysis. Given the results of this work, it can be concluded that:

- The methodology predicted a behavior of the plates similar to that observed in other theoretical and experimental works. Particularly, the maximum deflection of the plates was detected at the leading edge.
- Deflections happened even at low flow rates, and the plates did not undergo an abrupt and catastrophic collapse at any velocity.
- The maximum deflection increased linearly with the square of the velocity ratio for fluid velocities less than and equal to the Miller's theoretical value. For velocities above this value, a nonlinear behavior was observed. This behavior indicated that structural changes were taking place in the plates.
- For fluid velocities greater than the Miller's velocity, an extra deflection peak was observed near the trailing edge of the plates.
- During the study, no plastic deformation of the plates was detected.
- The methodology presented herein allows predicting the fluid flow velocity or dynamic pressure that causes the onset of fuel plate collapse.
- The methodology showed to be robust, produced qualitatively valid results, and it will be possible to apply it to study more complex configurations with several fuel plates.
- In this study, the prediction of the onset of hydroelastic instability by the numerical model matched with the velocity value calculated by the Miller's method. However, it is noteworthy that for other geometrical configurations and material properties this coincidence may not happen because the Miller's method is very simplified and the methodology proposed here is more detailed.

Acknowledgements

The authors acknowledge the financial support given by CAPES agency for the development of this research work.

Appendix A. Supplementary data

Supplementary data associated with this article can be found, in the online version, at http://dx.doi.org/10.1016/j.nucengdes.2018.04.009.

References

Alvim de Castro, A.J., 2017. Experimental Analysis of Critical Velocity in Flat Plate Fuel Element for Nuclear Research Reactors (Ph.D. Dissertation). Instituto de Pesquisas Energéticas e Nucleares.

de Andrade, D.A., Angelo, G., Angelo, E., Di Giovanni Santos, P.H., Vaz, Branco, de Oliveira, F., Torres, W.M., Umbehaun, P.E., Batista De Souza, J.A., Belchior Junior, A., Sabundjian, G., de Carvalho Prado, A., 2015. A CFD numerical model for the flow distribution in a MTR fuel element. In: Proceedings of the 2015 International Nuclear Atlantic Conference – INAC. Brazilian Nuclear Energy Association, São Paulo, Brazil.

ANSYS Inc., 2017a. ANSYS CFX Documentation – Release 18.0.

ANSYS Inc., 2017b. ANSYS Mechanical Documentation – Release 18.0.

Benjamin, T.B., 1963. The threefold classification of unstable disturbances in flexible surfaces bounding inviscid flows. J. Fluid Mech. 16, 436. http://dx.doi.org/10.1017/S0022112063000884.

Cekirge, H.M., Ural, E., 1978. Critical coolant flow velocities in reactors having parallel fuel plates. Comp. Math. Appl. 4, 153–156. http://dx.doi.org/10.1016/0898-1221(78)90025-1.

Curtis, F.G., Ekici, K., Freels, J.D., 2013. Fluid-Structure Interaction Modeling of High-Aspect Ratio Nuclear Fuel Plates Using COMSOL. In: Proceedings of the 2013 COMSOL Conference. Boston, USA.

Davis, D.C., Scarton, H.A., 1985. Flow-induced plastic collapse of stacked fuel plates. Nucl. Eng. Des. 85, 193–200. http://dx.doi.org/10.1016/0029-5493(85)90286-9.

Doan, R.L., 1958. The engineering test reactor – a status report. Nucleonics 16.

Du, Y., 2010. Numerical Simulation Of Mechanical and Thermal Fluid–Structure Interaction in Labyrinth Seals (PhD Dissertation). Technischen Universitat Darmstadt.

Gong, D., Huang, S., Wang, G., Wang, K., 2015. Heat transfer calculation on plate-type fuel assembly of high flux research reactor. Sci. Technol. Nucl. Install. 2015, 1–13. http://dx.doi.org/10.1155/2015/198654.

González Mantecón, J., Mattar Neto, M., 2017. Simplified CFD model of coolant channels typical of a plate-type fuel element: an exhaustive verification of the simulations. In: Proceedings of the 2017 International Nuclear Atlantic Conference – INAC. Brazilian Nuclear Energy Association, Belo Horizonte, Brazil.

Groninger, R.D., Kane, J.J., 1963. Flow induced deflections of parallel flat plates. Nucl. Sci. Eng. 16, 218–226. http://dx.doi.org/10.13182/NSE63-A26503.

Guo, C.Q., Païdoussis, M.P., 2000. Analysis of hydroelastic instabilities of rectangular parallel-plate assemblies. J. Pressure Vessel Technol. 122, 502–508. http://dx.doi.org/10.1115/1.1286019.

Howard, T.K., Marcum, W.R., Jones, W.F., 2015. A novel approach to modeling plate deformations in fluid–structure interactions. Nucl. Eng. Des. 293, 1–15. http://dx.doi.org/10.1016/j.nucengdes.2015.06.010.

INVAP, 2013. Brazilian Multipurpose Reactor Project – Core Thermal-Hydraulic Design in Forced Convection. Report RMBP-0130-2IIIN-005-A.

Jensen, P., Marcum, W.R., 2014. Predicting critical flow velocity leading to laminate plate collapse - flat plates. Nucl. Eng. Des. 267, 71–87. http://dx.doi.org/10.1016/j.nucengdes.2013.11.071.

Jesse, C.J., 2015. Analysis of the Potential for Flow-induced Deflection of Nuclear Reactor Fuel Plates Under High Velocity Flows (MSc Thesis). University of Missouri.

Johansson, E.B., 1959. Hydraulic Instability of Reactor Parallel-plate Fuel Assemblies. Report KAPL-M-EJ-9.

Kennedy, J., Solbrekken, G.L., 2011. Coupled hydro-mechanical analysis of U-10Mo fuel plates for manufacturing tolerance risk assessment. Proceedings of the 2011 European Research Reactor Conference – RRFM. European Nuclear Society, Rome, Italy.

Kennedy, J.C., 2015. Development and Experimental Benchmarking of Numeric Fluid Structure Interaction Models for Research Reactor Fuel Analysis (PhD Dissertation). University of Missouri.

Kim, G., Davis, D.C., 1995. Hydrodynamic instabilities in flat-plate-type fuel assemblies. Nucl. Eng. Des. 158, 1–17. http://dx.doi.org/10.1016/0029-5493(95)01023-B.

Li, Y., Lu, D., Zhang, P., Liu, L., 2012. Experimental investigation on fluid–structure interaction phenomenon caused by the flow through double-plate structure in a narrow channel. Nucl. Eng. Des. 248, 66–71. http://dx.doi.org/10.1016/j.nucengdes.2012.03.043.

Liu, L., Lu, D., Li, Y., Zhang, P., Niu, F., 2011. Large-amplitude and narrow-band vibration phenomenon of a foursquare fix-supported flexible plate in a rigid narrow channel. Nucl. Eng. Des. 241, 2874–2880. http://dx.doi.org/10.1016/j.nucengdes.2011.05.001.

Marcum, W.R., 2014. Predicting critical flow velocity leading to laminate plate collapse - Cylindrical plates. Nucl. Eng. Des. 278, 50–63. http://dx.doi.org/10.1016/j.nucengdes.2014.07.015.

Miller, D.R., 1958. Critical Flow Velocities for Collapse of Reactor Parallel-plate Fuel Assemblies. Report KAPL-1954. doi:https://doi.org/10.2172/4199355.

Oberkampf, W.L., Roy, C.J., 2010. Verification and Validation in Scientific Computing. Cambridge University Press, New York.

Pavone, S.J., Scarton, H.A., 1983. Laminar flow induced deflections of stacked plates. Nucl. Eng. Des. 74, 79–89. http://dx.doi.org/10.1016/0029-5493(83)90141-3.

Perrotta, J.A., Soares, A.J., 2015. RMB: The New Brazilian multipurpose research reactor. Int. J. Nucl. Power 60, 30–34.

Pozarlik, A.K., Kok, J.B.W.K., 2007. Numerical Investigation of One- and Two-Way Fluid-Structure Interaction in Combustion Systems. In: Proceedings of the International Conference on Computational Methods for Coupled Problems in Science and Engineering – COUPLED PROBLEMS 2007. Barcelona, Spain.

Rao, A., 2003. Fluid-solid interaction analysis using ANSYS/multiphysics. In: Computational Fluid and Solid Mechanics. Elsevier, pp. 1492–1496. http://dx.doi.org/10.1016/B978-008044046-0.50364-X.

Salama, A., El-Amin, M.F., Sun, S., 2015. Three-dimensional, numerical investigation of flow and heat transfer in rectangular channels subject to partial blockage. Heat Transf. Eng. 36, 152–165. http://dx.doi.org/10.1080/01457632.2014.909191.

Salim, S.M., Cheah, S.C., 2009. Wall y+ strategy for dealing with wall-bounded turbulent flows. In: Proceedings of the International MultiConference of Engineers and Computer Scientists – IMECS 2009. Hong Kong, Hong Kong.

Scavuzzo, R.J., 1965. Hydraulic instability of flat parallel-plate assemblies. Nucl. Sci. Eng. 21, 463–472. http://dx.doi.org/10.13182/NSE65-A18790.

Smissaert, G.E., 1969. Static and dynamic hydroelastic instabilities in MTR-type fuel elements part II. Theoretical investigation and discussion. Nucl. Eng. Des. 9, 105–122. http://dx.doi.org/10.1016/0029-5493(69)90052-1.

Smissaert, G.E., 1968. Static and dynamic hydroelastic instabilities in MTR-type fuel elements Part I. Introduction and experimental investigation. Nucl. Eng. Des. 7, 535–546. http://dx.doi.org/10.1016/0029-5493(68)90103-9.

Smith, R.L., 1968. Dynamic Pressure Limits for Flat Plates as Related to Nuclear Fuel Elements. NASA Technical Note D-4417.

Stromquist, W.K., Sisman, O., 1948. High Flux Reactor Fuel Assemblies Vibration and Water Flow.

Swinson, W.F., Battiste, R.L., Luttrell, U., Yahr, G.T., 1995. An experimental investigation of the structural response of reactor fuel plates. Experim. Mech. 212–215. http://dx.doi.org/10.1007/BF02319660.

Swinson, W.F., Yahr, G.T., 1990. Dynamic pressure approach to analysis of reactor fuel plate stability. In: 1990 ANS Annual Meeting, Nashville, USA.

Timoshenko, S.P., Woinowsky-Krieger, S., 1959. Theory of Plates and Shells, Second ed. McGraw-Hill Book Company, Inc.

Weaver, D.S., Unny, T.E., 1970. The hydroelastic stability of a flat plate. J. Appl. Mech. 823–827. http://dx.doi.org/10.1115/1.3408615.

White, F.M., 2011. Fluid Mechanics, Seventh ed. McGraw-Hill, New York.